Amino Acids (2010) 38:1595–1605
DOI 10.1007/s00726-009-0376-y

ORIGINAL ARTICLE

# Metabolic stability of human parathyroid hormone peptide hPTH (1–34) in rat tissue homogenates: kinetics and products of proteolytic degradation

**Sha Liao · Jian-Kun Qie · Ming Xue · Zhen-Qing Zhang · Ke-Liang Liu · Jin-Xiu Ruan**

Received: 21 July 2009 / Accepted: 13 October 2009 / Published online: 6 November 2009


**Abstract** The present study aim to investigate the metabolic stability and degradation of cleavage sites of human parathyroid hormone peptide, hPTH (1–34), in rat tissue homogenate, and to identify the types of proteases involved in hPTH (1–34) processing degradation. The stability of hPTH (1–34) in rat kidney, lung and liver homogenates was evaluated by LC–ESI–MS, and the structures of the major degradation products were identified by MALDI–TOF MS and LC–ESI–MS/MS. The ability of protease inhibitors to inhibit hPTH (1–34) degradation was used to identify the class of proteases involved in the metabolism of hPTH (1–34). hPTH (1–34) peptide was readily degraded in rat kidney, liver, and lung homogenates, with half-lives of 5.7, 32.2, and 18.9 min, respectively. The degradation of hPTH (1–34) in each tissue can be inhibited by inhibitors of serine and metalloproteases. The major degradation products of hPTH (1–34) are similar in each tissue and suggest that hPTH (1–15) and hPTH (16–34) appear as the major degradation products. The degradation patterns of hPTH (1–34) incubated in rat kidney, liver and lung homogenates are largely overlapping, and a majority of the fragments are generated via cleavages at sites of Leu15–Asn16 peptide bond.

**Keywords** Human parathyroid hormone · Degradation · Cleavage site · Mass spectrometry · Enzyme inhibitors

S. Liao and J.-K. Qie contributed equally to this work.

**Electronic supplementary material** The online version of this article (doi:10.1007/s00726-009-0376-y) contains supplementary material, which is available to authorized users.

S. Liao · J.-K. Qie · M. Xue · Z.-Q. Zhang (✉) · K.-L. Liu (✉) · J.-X. Ruan
Beijing Institute of Pharmacology and Toxicology, 27 Taiping Road, Haidian District, 100850 Beijing, People's Republic of China
e-mail: zqzhang55@yahoo.com

K.-L. Liu
e-mail: keliangliu@yahoo.com

M. Xue
Department of Pharmacology, Capital Medical University, 100069 Beijing, People's Republic of China

## Introduction

The use of pharmacokinetic analysis to guide and expedite drug development has received increasing interest in recent years (Galluppi et al. 2001). Although pharmacokinetic principles have been widely used in the development of traditional low molecular weight chemical drugs, there has been a growing number of reports describing the metabolic stability and biological processing of therapeutic peptides (Föger et al. 2008). During systemic circulation, enzymatic degradation of peptides in the blood, liver, lung and kidney (Werle and Bernkop-Schnurch 2006), together with fast renal clearance, generally results in short peptide half-lives that limit their therapeutic activity. To improve their therapeutic potential, it will be important to thoroughly characterize the metabolic processing of peptides and establish quantitative structure–stability relationships that can be used to design peptide-based therapeutics with increased metabolic stability (Vergote et al. 2008).

Osteoporosis is a silent disease that affects millions of people worldwide (Hamdy 2002). While not immediately life threatening, the mortality rate for women 1 year after an osteoporotic hip fracture is one in five, which is similar to breast cancer mortality rates; the mortality rate for men is even worse (Seeman et al. 2007; Fraenkel et al. 2007). New

bone formation and reposition during normal bone remodeling is regulated, in part, by calcium and phosphate levels. Calcium and phosphate homeostasis in the blood and bones is maintained by human parathyroid hormone (hPTH (1–84)), an 84-amino acid (9.5 kDa) endogenous polypeptide (Potetinova et al. 2006). hPTH has long been recognized for its ability to stimulate new bone formation (Reeve 2002), and in 2002, a peptide comprised of the amino-terminal 34 amino acids of hPTH, denoted hPTH (1–34) (Fig. 1), was approved by the U.S. Food and Drug Administration as the first anabolic agent that actually stimulates new bone formation (Quattrocchi and Kourlas 2006).

Early pharmacokinetics studies of hPTH (1–34) demonstrated a dose linearity of the pharmacokinetics over a s.c. dosage range from 5 to 20 μg/kg in healthy rats and it is rapidly absorbed and eliminated with the accumulation of hPTH (1–34) in tissues/organs which examined to be low (Hu et al. 2006). Chu et al. (2007) mentioned that when administered by i.v., $t_{1/2\beta}$ of it in serum was only 5 min in human. More PK investigations in different animal species (rat, dog and monkey) following i.v. administration (Jones et al. 2006) also confirmed the rapid elimination of hPTH (1–34) in vivo process ($t_{1/2\beta}$ is 5–25 min). Previous in vivo studies showed $^{125}$I-hPTH (1–34) underwent a rapid and wide distribution in rat, and the substantial disposition is in the lung (the highest radioactivity level, 90 ± 12% ID/g), kidney (59 ± 10%) and liver (Hu et al. 2006), which is similar to the previous report on the distribution of $^{125}$I-labeled hPTH (1–84) after i.v. injection in rats (Neuman et al. 1975). It was proposed that the short elimination half-life is primarily due to degradation of the peptide in these organs, which were recognized to be the main organs for pharmacological active site and metabolism/elimination of hPTH (1–34) in vivo (Daugaard et al. 1994a, b). Further detailed in situ evidence came from Daugaard et al. using an isolated perfused rat kidney and liver model confirmed the rapid and extensive metabolism of hPTH (1–34), with the metabolism and/or clearance principally in renal by mechanisms of peritubular uptake with subsequent re-absorption (Daugaard et al. 1994a, b; Jones et al. 2006). Rouleau et al. and Jones et al. also observed the central role of the liver in clearing this peptide from plasma by a hepatocyte internalization mechanism (Jones et al. 2006).

The unique properties of these organs, suggested that more detailed chemical examination of these proteolytic events at the subcellular level would provide information physiologically relevant to the peripheral metabolism of hPTH (1–34) in the intact animal and this process may be important to understanding the role of hPTH (1–34) metabolism in calcium homeostasis. Therefore, in this study, we have characterized the in vitro metabolic stability of hPTH (1–34) in homogenates of rat liver, kidney, and lung tissues. The degradation of hPTH (1–34) in the three tissue homogenates was monitored as a function of time, and the major degradation products were identified by LC–ESI–MS/MS and matrix-assisted laser desorption/ionization time-of-flight mass spectrometry (MALDI–TOF MS). In addition, we characterized the effect of standard protease inhibitors on hPTH (1–34) stability to identify the enzymes involved in hPTH (1–34) degradation. These results provide a basis for the design of hPTH (1–34) analogues that have improved metabolic stability.

## Methods

### Materials

hPTH (1–34) peptide (4118 Da) was synthesized by our institute, purified by HPLC (>99% purity), and stored at −70°C. Acetonitrile, methanol and formic acid (99%, HPLC grade) were obtained from Fisher (Fair Lawn, NJ). Analytical grade trifluoroacetic acid (TFA) was purchased from Sigma (St. Louis, MO). HPLC grade water was doubly purified with a Milli-Q system (Millipore, Molsheim, France). Peptidase inhibitors were obtained from MERCK (Darmstadt, Germany). All other reagents were of the highest grade commercially available.

### Preparation of tissue homogenates

Five male Sprague–Dawley rats weighing 240–260 g were purchased from the Beijing Vital River Laboratories (Beijing, China). Prior to the study, the animals were fasted overnight with free access to water, exsanguinated and decapitated. The lungs, livers and kidneys were isolated from each rat, washed in ice-cold saline solution (0.9% sodium chloride), trimmed of adhering tissue and immediately collected. The excised tissue was weighed, cut into small pieces, and 4 mL of ice-cold incubation buffer (50 mM Tris–HCl pH 7.4) was added per 1 g of tissue. For each tissue, samples from the five rats were pooled and homogenized using a Teflon digital homogenizer. The homogenates were

Ser$^{1}$-Val-Ser-Glu-Ile$^{5}$-Gln-Leu-Met-His-Asn$^{10}$-Leu-Gly-Lys-His-Leu$^{15}$-Asn-Ser-Met-Glu-Arg$^{20}$-Val-Glu-Trp-Leu-Arg$^{25}$-Lys-Lys-Leu-Gln-Asp$^{30}$-Val-His-Asn-Phe$^{34}$-OH

rhPTH (1-34) (teriparatide)

**Fig. 1** The amino acid sequence of recombinant human parathyroid hormone (1–34)

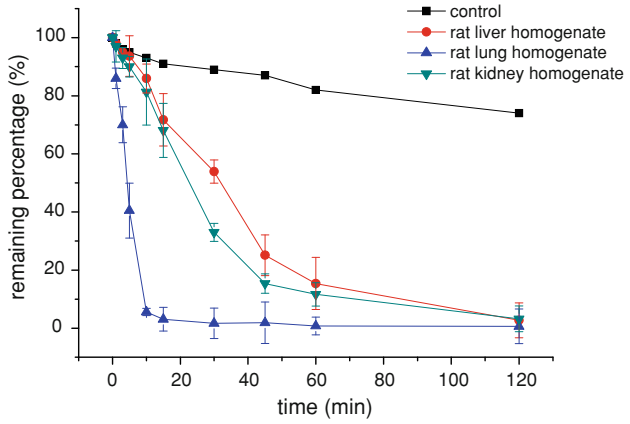


**Fig. 2** Stability of hPTH (1–34) in rat liver, lung and kidney homogenates. Residual rates of hPTH (1–34) at 0 min were considered 100%, and hPTH (1–34) solutions without homogenate were used for the control. $n = 3$

**Table 1** Degradation of hPTH (1-34) in rat tissue homogenates at pH 7.4 and 37°C

| Tissue homogenate | Half-lives (min) |
|---|---|
| Kidney | 5.5 ± 0.32 |
| Liver | 32.2 ± 5.5 |
| Lung | 18.9 ± 3.6 |

The rate constants of degradation were estimated by non-linear Michaelis–Mente model

centrifuged (2,000*g*) for 10 min at 4°C, and the supernatants were stored at −80°C until further analysis. In vitro assays were performed within 8 days of tissue collection.

The total protein concentration in the tissue homogenates was determined using the bicinchoninic acid (BCA) colorimetric assay (Pierce Biotechnology, Rockford, IL, USA) with bovine serum albumin as a reference standard. Homogenates were diluted to 2.5 mg protein/ml as necessary.

## Degradation of hPTH (1–34) in tissue homogenates

Degradation of hPTH (1–34) was measured following incubation with rat lung, kidney and liver homogenates. Reactions were initiated by addition of hPTH (1–34) at a final concentration of 10 µM. Samples (50 µl) were withdrawn at different time intervals (0, 1, 3, 5, 10, 15, 30, 45,

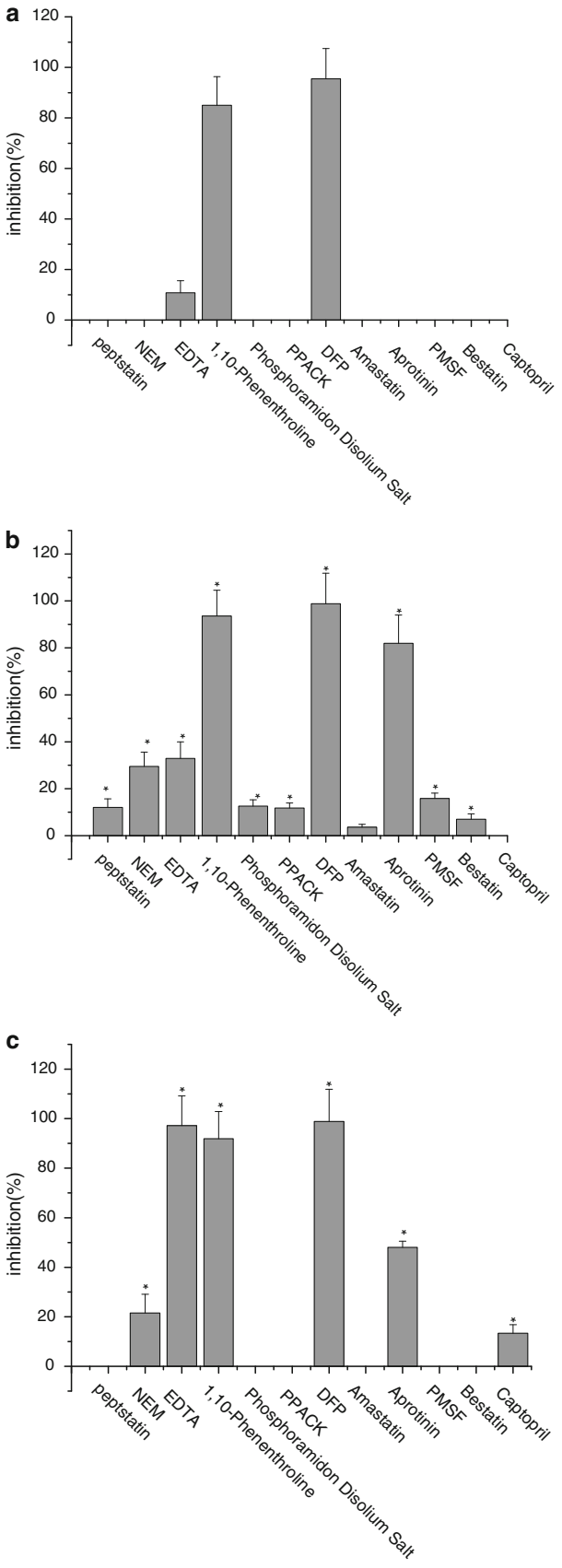


**Fig. 3** Effect of protease inhibitors on hPTH (1–34) degradation. The ▶ inhibition of hPTH (1–34) degradation was measured in rat **a** kidney, **b** lung, and **c** liver pre-treated with indicated protease inhibitor. The amount of peptide remaining was assayed after (kidney) 30 min or (lung, liver) 60 min. The results are expressed as the percentage of inhibition of hPTH (1–34). $n = 3$; $^*P < 0.05$; compared with the control group

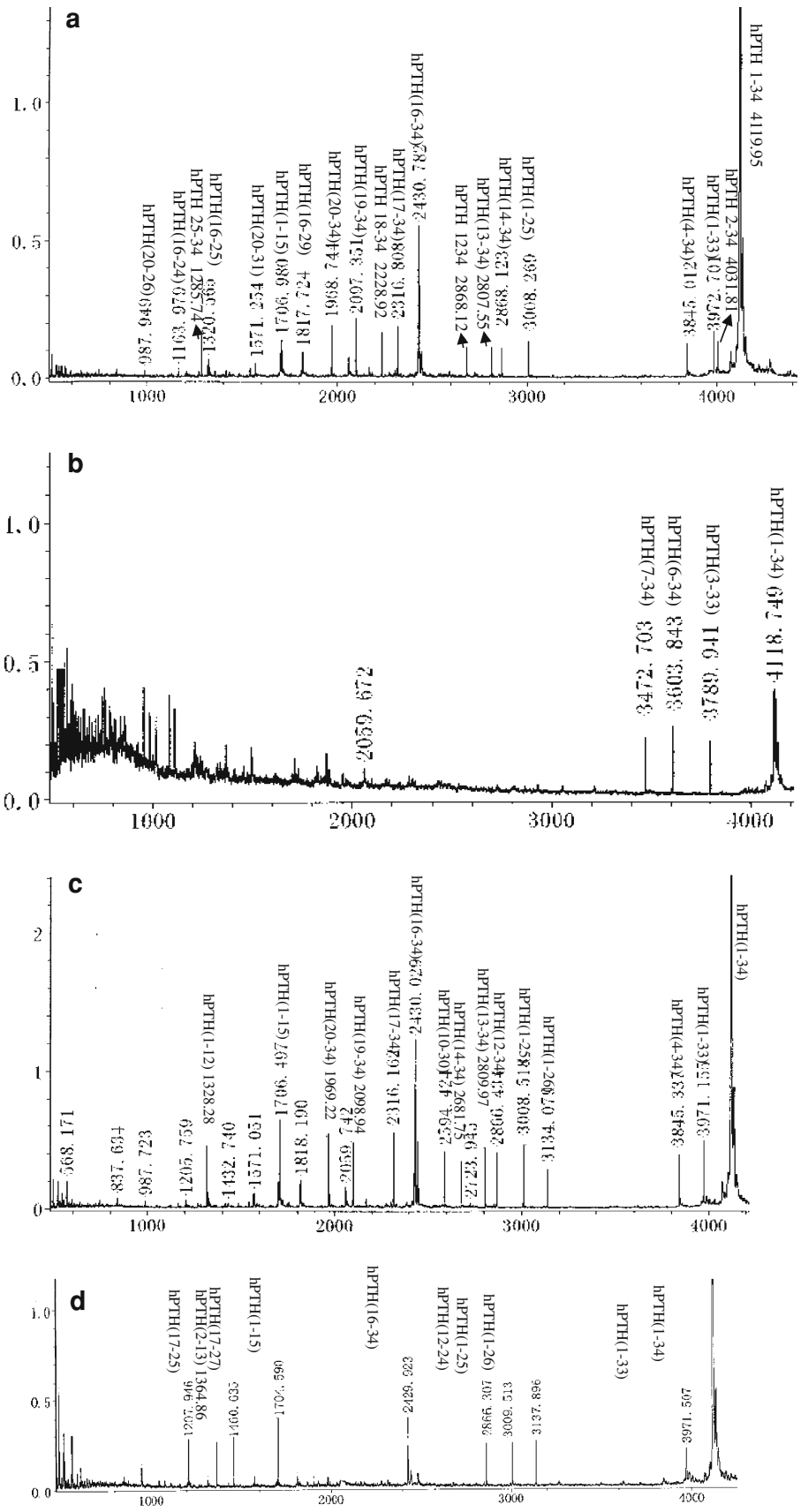


**Fig. 4** MALDI–TOF MS spectrum of degradation products from hPTH (1–34) incubated in rat kidney homogenate for **a** 10 min and **b** 60 min, liver homogenate for **c** 10 min, and lung homogenate for **d** 30 min, respectively


**Fig. 5** Proposed scheme for metabolic cleavage site of hPTH (1–34) in rat **a** kidney, **b** liver, and **c** lung homogenates. *Arrowheads* indicate cleavage sites in hPTH; *solid arrowheads*, sites of concomitantly detected N- and C-terminal counterparts; *open arrowheads*, only N-terminal fragment detected; *up-arrowheads*, only C-terminal fragment detected. *Grey* symbols indicate cleavage sites that are targeted at the onset of incubation. *Black* symbols indicate cleavage sites that are targeted in major metabolites or intact hPTH (1–34) by sequential cleavage of aminopeptidase or carboxypeptidase activity

60, 90, 120, 240 and 360 min) at 37°C water bath, immediately mixed with three volumes of ice-cold methanol to terminate enzymatic activity and vortexed. The mixtures were centrifuged at 10,000*g* for 10 min at 4°C; the resulting supernatants were dried with a Speed Vac and stored at −20°C until further analysis.

The dried residue was re-dissolved in 50 μL of HPLC mobile phase (50/50 (v/v) ACN/H2O, 0.1% (w/v) FA) and analyzed by LC–ESI–MS and LC–ESI–MS/MS for characterization of the stability and identification of metabolites, respectively. For MALDI–TOF MS analysis, the samples were mixed with the MALDI matrix and subjected to MALDI–MS target for mass spectral analysis. Appropriate blanks, controls (i.e. no protein) and reference solutions were prepared in a similar manner. Half-life decay rates were derived by fitting non-linear Michaelis-Mente model to the measured metabolic stability as a function of time.

## Inhibition of hPTH (1–34) metabolism

The following protease inhibitors and concentrations were tested for their ability to increase hPTH (1–34) metabolic stability: Pepstatin (aspartic protease inhibitor, 0.5 mM), NEM (cysteine protease inhibitor, 10 mM), leuhistin (cysteine protease inhibitor, 83 μM), EDTA (metalloprotease inhibitor, 10 mM), phenenthroline (metalloprotease inhibitor, 2 mM), phosphoramidon disodium salt (neutral endopeptidase; thermolysin inhibitor, 92 μM), PPACK (dipeptidyl peptidase IV; thrombin inhibitor, 210 μM), soybean (trypsin inhibitor, 50 μM), DL-Thiorphan (Endo-24.11 inhibitor, 2 mM), captopril (angiotensin-converting enzyme inhibitor, 30 μM), diisopropylfluorophosphate (DFP) (serine protease inhibitor, 10 mM), Aprotinin (serine proteases inhibitor 0.32 mM), PMSF (serine protease inhibitor 1 mM), amastatin (aminopeptidases inhibitor 100 μM), bestatin (aminopeptidases inhibitor 2 mM). Protease inhibitors at the indicated concentrations were individually added to diluted homogenates, vortexed, and pre-incubated for 10 min at 37°C. Each pre-treated biological matrix was incubated with hPTH (1–34) (10 μM final concentration) for an additional 30 min (kidney) or 60 min (liver and lung) at 37°C and compared to similar preparations containing no enzyme inhibitor and to synthetic peptide incubated for 0 min. Samples were treated and analyzed as described above.

## Mass spectrometry

A triple-stage quadruple mass spectrometer (TSQ Quantum Discovery, Thermo Electron, San Jose, CA) equipped with an atmospheric ionization (API) source was used for detection of intact hPTH (1–34). Electrospray LC–MS was

performed in positive-ion selected ion monitoring (SIM) mode. Both Finnigan Surveyor™ HPLC system and Finnigan TSQ Quantum Discovery were controlled using Xcalibur® version 1.4 software. The other mass spectrometer parameters were as follows: ESI Needle Voltage: 4,500 V; Nitrogen Sheath Gas Pressure: 35 arb units; Auxillary Gas Pressure: 5 arb units; Ion Transfer Capillary Temperature: 250°C; Tube Lens Offset: −90 V (at *m/z* 849); Source CID Offset: 7 V. LC experiments were conducted using a Finnigan Surveyor™ HPLC system (Thermo Electron). Separation of hPTH (1–34) was achieved using a 100 × 2.1 mm SB300C18 column (Agilent, USA) packed with on-line filters. Mobile phase compositions were (A) 0.1% (v/v) formic acid (FA) in water and (B) acetonitrile. Samples were eluted with a linear gradient from 15% B at $t = 0.0$ min to 70% B at $t = 10.0$ min. After a 1 min hold at 70% B, the column was recycled to 15% B and re-equilibrated for 10 min. The flow rate during the gradient separation was 0.2 mL/min. The injection volume for all LC experiments was 10 μL.

A ThermoFinnigan LCQ mass spectrometer (ThermoFinnigan, CA) was used to analyze the degradation products of hPTH (1–34). The residue was re-dissolved in a small volume of the HPLC mobile phase and analyzed by LC–ESI–MS/MS to detect the metabolites (scanning range *m/z* 300–1,700). The same LC–MS operating conditions described above were used with the following modification of the elution method. The column was equilibrated in a formic acid (FA)/water mixture (mobile phase A). Samples were eluted with a linear gradient of mobile phase B (formic acid/acetonitrile, 0.1% v/v) from 0 to 70% over a 45 min period. The Bioworks (3.3.1, Thermo) protein analysis software was used to search for the peptide fragments in the ions of each peak.

Metabolites emerging from the degradation of hPTH (1–34) were also analyzed by MALDI–TOF MS carried out in the linear positive ion mode on a Bruker REFLEX III MALDI–TOF mass spectrometer (Bruker-Franzen, Bremen, Germany). Samples were mixed with an equal volume of matrix solution (α-cyano-4-hydroxycinnamic acid) using the dried-droplet technique. External mass calibration of the mass spectrometer was performed with bradykinin, human secretin and ubiquitin peptide standards (Sigma, St Louis, MO).

### Statistical analysis

Results from individual experiments are presented as the mean ± standard error. Peptide degradation experiments were collected in graphs reporting the amount of peptide remaining (area %) versus time. Each hydrolysis experiment was repeated three times in duplicate and reported as the mean value. The statistical significance was determined by analysis of variance (ANOVA) followed by Student–Newman–Keuls test. A probability level of $p < 0.05$ was used to indicate statistical significance.

## Results

The metabolic stability of hPTH (1–34) in homogenates of rat liver, lung, and kidney tissue is shown in Fig. 2. hPTH (1–34) was monitored over a period of 120 min in each matrix. After 30 min, approximately 51 and 30% of the starting hPTH (1–34) peptide remained in liver and lung homogenates, respectively. In contrast, hPTH (1–34) was almost completely degraded within 30 min (~2.6% remaining) in kidney homogenate; no degradation was

**Table 2** MALDI–TOF MS peak spectrum of liver homogenate metabolites, $(M + H)^+$, of hPTH (1–34)

| Peak no. | MALDI | ESI | Fragments |
|---|---|---|---|
| 1 | 1,272.6 | 1,269.6 | 1–11 |
| 2 | 1,320.4 | | 4–14 |
| 3 | | 1,326.6 | 1–12 |
| 4 | 1,413.9 | | 21–31 |
| 5 | 1,433.7 | | 4–15 |
| 6 | 1,542 | | 13–24 |
| 7 | 1,570.8 | 1,568.4 | 20–31 |
| 8 | 1,583.9 | | 23–34 |
| 9 | 1,601.1 | | 19–30 |
| 10 | 1,698.9 | 1,696.8 | 19–31 |
| 11 | 1,705 | 1,704.8 | 1–15 |
| 12 | 1,755.8 | | 12–25 |
| 13 | 1,817.7 | 1,816.4 | 16–29 |
| 14 | 1,984.2 | | 10–25 |
| 15 | 2,098 | | 19–34 |
| 16 | 2,229.7 | | 18–34 |
| 17 | 2,284.3 | 2,281 | 16–33 |
| 18 | 2,315.2 | 2,314.3 | 17–34 |
| 19 | 2,431.7 | 2,428.9 | 16–34 |
| 20 | 2,445.5 | | 5–24 |
| 21 | 2,682.5 | | 14–34 |
| 22 | 2,810 | | 13–34 |
| 23 | 2,866.6 | | 12–34 |
| 24 | 3,009 | | 1–25 |
| 25 | 3,136 | | 1–26 |
| 26 | 3,508.4 | | 1–29 |
| 27 | 3,623.5 | | 1–30 |
| 28 | 3,845.3 | | 4–34 |
| 29 | 4,119.2 | 4,115.9 | 1–34 |

The initial hPTH (1–34) concentration of the respective metabolism experiment was 10 μM. The incubation time was 45 min. For comparison, the data of the corresponding ESI–MS experiment is also included

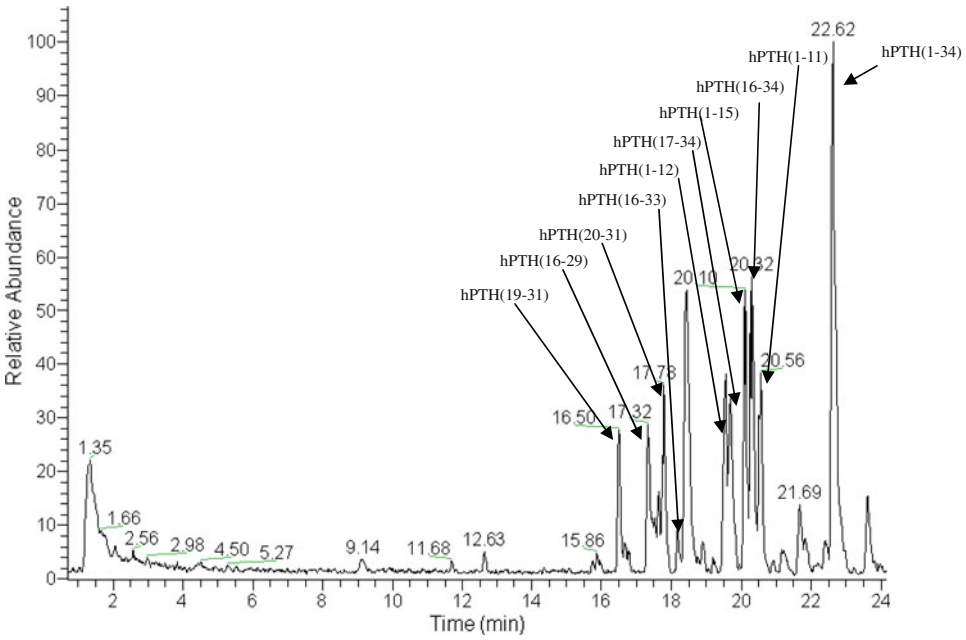


**Fig. 6** LC–ESI–MS chromatographic profile of hPTH (1–34) metabolites following incubation in rat liver homogenate for 45 min

observed in control experiments over the 120 min incubation period. The half-life values for degradation of hPTH (1–34) in the three matrices were extracted from non-linear Michaelis–Mente model fits to the stability profile (Table 1). The rank order of degradation rate of hPTH (1–34) in the three biological matrices was kidney > lung > liver, with the half-life of 5.5, 18.9 and 32.2 min, respectively.

To identify the types of proteolytic enzymes involved in hPTH (1–34) metabolism, various protease inhibitors (Fig. 3) were screened for their ability to inhibit degradation of hPTH (1–34) in rat tissue homogenates over a 60 min (lung and liver) or 30 min (kidney) period. In all three contexts, 1,10-phenenthroline and DFP inhibited hPTH (1–34) degradation to a similar extent (>80%). EDTA also inhibited degradation in all three contexts, but in a tissue-specific manner with inhibition being greatest in the liver (97%) and weakest in the kidney (11%). Aprotinin and NEM had a significant inhibitory effect on degradation of hPTH (1–34) in the lung and liver, but no inhibition was observed in the kidney. Captopril had a mild inhibitory effect (13%) in the liver. The remaining inhibitors had mild effects on the stability of hPTH (1–34) in the lung, but no effect in the liver or kidney homogenates. These results are summarized in Fig. 3.

The hPTH (1–34) degradation products were identified by MALDI–TOF MS. After 10 min incubation in kidney homogenate, a number of fragments were observed (Fig. 4a). The N-terminal metabolite hPTH (1–15) and its C-terminal counterpart hPTH (16–34) were detected and result from cleavage at the Leu15–Asn16 peptide bond. Additional fragments observed after 10 min include hPTH (2–34), hPTH (4–34), hPTH (12–34), hPTH (13–34), hPTH (14–34), hPTH (17–34), hPTH (18–34), hPTH (19–34), hPTH (20–34), hPTH (25–34), hPTH (1–33), and hPTH (1–25); their respective N- or C-terminal degradation counterparts were not detected. Although initially present after 10 min, the two early and major degradation products hPTH (1–15) and hPTH (16–34) were not detected after 60 min (Fig. 4b), suggesting that they were further degraded. These major fragments were also confirmed by LC–ESI–MS/MS (Supplement material). Figure 5a illustrates a summary of the suggested cleavage sites of hPTH (1–34) in contact with rat kidney homogenate.

Similar degradation products of hPTH (1–34) were observed following incubation in rat liver homogenate (Fig. 4c), with 11 of the 13 identified metabolites identical to those identified after incubation with rat kidney. Masses of fragments identified by MALDI–TOF MS following a 45 min incubation of hPTH (1–34) with rat liver is shown in Table 2. After 10 min, the initial cleavage sites were found between residues Leu15–Asn16, Ser3–Glu4, and Asn33–Phe34 (Fig. 4c). Additional fragments resulting from sequential cleavage of aminopeptidase or carboxypeptidase activity were hPTH (4–34), hPTH (12–34), hPTH (13–34), hPTH (14–34), from the N-terminal of hPTH (1–34); hPTH (1–33), hPTH (1–25), hPTH (1–26) from the C-terminal of hPTH (1–34); hPTH (1–12) from hPTH (1–15); hPTH (17–34), hPTH (19–34), hPTH (20–34) from hPTH (16–34). The main products of hPTH (1–34) metabolism in rat lung (Fig. 4d) are similar to those observed following degradation in the liver.

A representative chromatogram of hPTH (1–34) degradation products in liver homogenate after 45 min incubation is shown in Fig. 6 (major products shown), and a CID

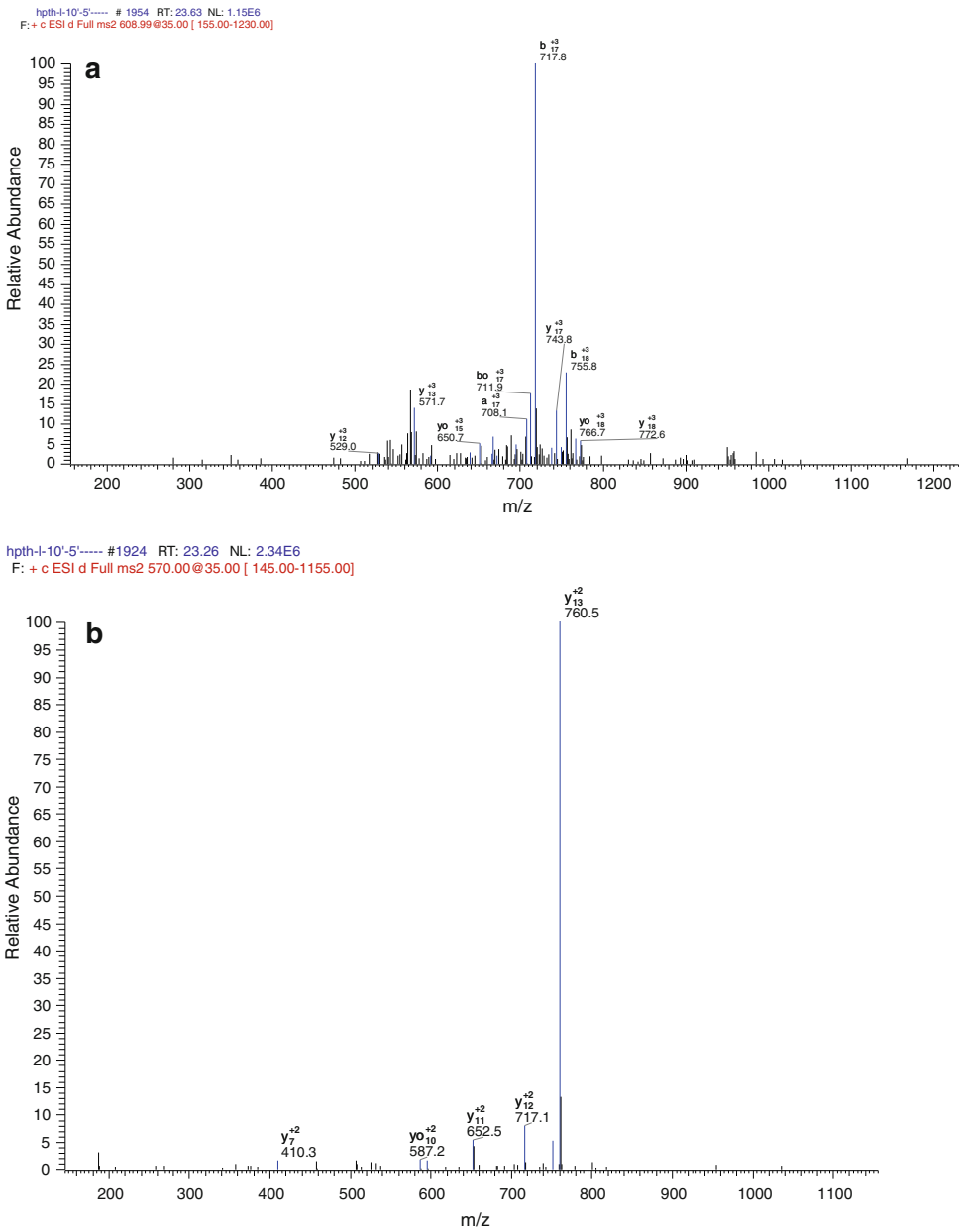


**Fig. 7** Tandem CID mass spectrum of the doubly protonated peptide **a** hPTH (16–34) and **b** hPTH (1–15). Precursor ions were generated by electrospray ionization using the on-line LC–ESI/MS–MS procedure described in "Methods"

spectrum of the two main degradation fragments of hPTH (1–34) is shown in Fig. 7. One metabolite showing an $(M + H)^+$ with *m/z* 2,430 was identified as the hPTH (16–34) peptide fragment; the fragment hPTH (1–15) can be ruled out from the series y10 to y13. Other metabolites of hPTH (1–34) were confirmed in this manner, and their amino acid sequences were determined by LC–ESI–MS/MS. This procedure was used to assign the fragments listed in Table 2. Summary of the metabolic fate of hPTH (1–34) in contact with rat liver homogenate detected by LC–ESI–MS/MS is presented in Fig. 8. hPTH (1–34) degraded overtime until it was essentially undetected by 120 min. The primary degradants, hPTH (1–15) and hPTH (16–34) increased in concentration over the first 20 min, held at a relatively steady amount over the next 20 min, and then decreased until undetectable by 120 min. The rat liver homogenate digested hPTH (1–34) and its putative degradants to ~100% completion.

## Discussion

In this study, we have investigated the metabolism of hPTH (1–34) in homogenates from rat liver, kidney and lung. Our study has demonstrated that this peptide is rapidly metabolized by enzymes associated with all the three tissue homogenates, and this metabolism is most likely due to serine proteases and metalloproteases in rat kidney and

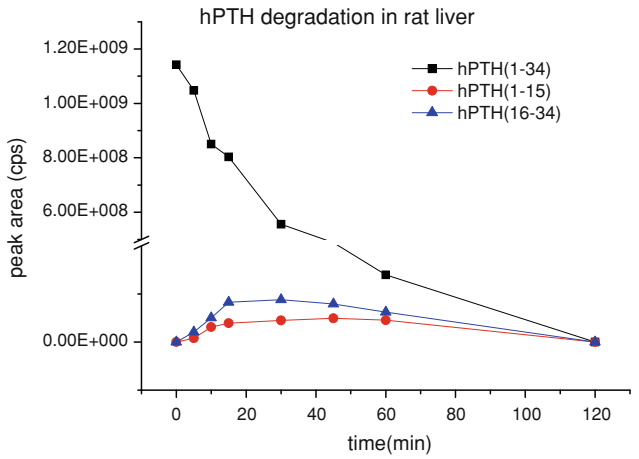


**Fig. 8** Time course of hPTH (1–34) degradation by rat liver homogenate in vitro. $n = 3$; $^*P < 0.05$; compared with the control group

liver, with additional contributions from aspartic proteases, cysteine proteases, and neutral endopeptidase in the lung. hPTH (1–34) is the first approved anabolic agent for osteoporosis treatment. Modifications of hPTH (1–34) that result in prolonged biological half-life (e.g. stabilization towards exo- and endopeptidases) are deemed necessary to improve its therapeutic utility. To our knowledge, however, there are no data available on the both preclinical and clinical metabolism/degradation of this peptide. On the other hand, as most of our present knowledge about the PK of this peptide is based upon studies with it in rat species (Hu et al. 2006; Jones et al. 2006; Daugaard et al. 1994a, b), which give us very crucial and vital clue that plasma, kidney, liver and lung may be the key biological compartments and organs account for most of the distribution/degradation of hPTH (1–34), the present studies aim to further investigate and compare the tissue specific metabolism/elimination in terms of extent of degradation and the metabolic pattern of hPTH (1–34) in rat model. In addition, our preliminary experiments carried out with rat/human plasma and corresponding inactivated matrixes in vitro suggested that little degradation occurs in the circulation and that most of the peptide clearance seemed is more related with their target/distribution organs, e.g. kidney, liver and lung.

Homogenates represent an easy and reliable biological system for studies of peptide metabolism in multiple organs and/or across species (Liao et al. 2008; Ekins et al. 2000). In this system, enzymes from different metabolic compartments are mixed and expose the peptide substrate to enzymes that are more abundant than in the subcellular fractions isolated from organs. In vitro assays were developed in rat tissue homogenates to characterize the stability of hPTH (1–34) and identify intermediary degradation products. Rat kidney, liver and lung all degraded hPTH (1–34) readily, however, relative rates varied among tissues. After 30 min of incubation, hPTH (1–34) is broken down to the greatest extent in rat kidney. These differences may be due to the differential expression of enzyme and/or cofactors responsible for hPTH (1–34) degradation in the three tissues. Degradation of hPTH (1–34) was approximately 6 and 4-fold faster in kidney homogenate than in liver and lung, respectively. This phenomenon can be explained by the fact that the localization of the proteolytic enzymes is different in the particular tissue (Powell et al. 1992; Boulanger et al. 1992).

To identify the specific peptidase involved in the metabolism of hPTH (1–34), the peptide was incubated in the three different rat tissue homogenates in the presence of various general and specific protease inhibitors. In kidney, robust inhibition of hPTH (1–34) degradation was observed in the presence of 1,10-phenenthroline and DFP, which inhibit metallopeptidases and serinepeptidases, respectively. In liver, in addition to the inhibitors mentioned above, EDTA (metallopeptidase inhibitor) and Aprotinin (serinepeptidase inhibitor) also had a significant inhibitory effect. Additional enzyme inhibitors were found to inhibit degradation of hPTH (1–34) in rat lung. Out of all inhibitors that increase the metabolic stability of hPTH (1–34), however, inhibitors of serine and metallopeptidases are the most effective in the three tissue homogenates. This implies that metallopeptidases and serinepeptidases are

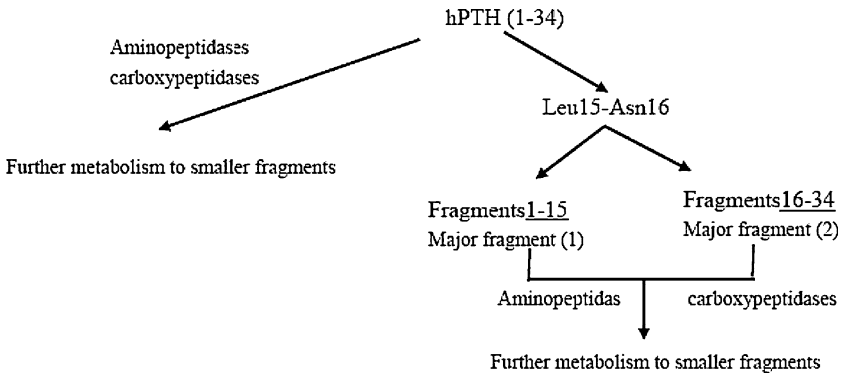


**Fig. 9** Putative pathway for degradation of Hpth (1–34) in rat liver, lung and kidney homogenates

most likely to be digestive enzymes in the three tissues in vivo.

Characterization of peptide stability and degradation is aided by recent advances in mass spectrometry (Van den Broek et al. 2008). In the present work, MALDI–TOF MS and LC–ESI–MS/MS were both applied to identify the hPTH (1–34) peptide fragments that resulted from enzymatic degradation in rat tissue homogenates. As shown in Table 2, the hPTH (1–34) metabolic cleavage products identified were similar with both techniques. However, some metabolites found with MALDI–TOF MS were not detected in ESI–MS/MS. These discrepancies, however, can be explained by differences in the study protocol. For MALDI–TOF MS, the native incubation solution was analyzed directly without further processing. This procedure resulted in higher metabolite concentrations compared to the precipitation and subsequent freeze drying of the incubation solutions prior to ESI–MS/MS analysis. On the other hand, the low concentration of some degradation products made it difficult, and in some cases impossible, to positively determine the amino acid sequence by MS/MS technology. Because of these low levels, it is likely that additional degradation products were formed below the limits of detection. However, by extract ions on different mass range, the assigned hPTH (1–34) peptide degradation sequences can be indicated at the individual mass traces and the primary degradation products' metabolic fate can be assumed. In order to avoid/minimize loss of analyze, beside polypropylene (PP), 50/50 (v/v) ACN/$H_2O$, 0.1% (w/v) FA was used to solve the samples and no significant peptide losses during speed-vac had been detected during our experiment setup. Our result is consistent with John et al.'s (2004) results, while it is not fully consistent with Pezeshki et al.'s (2009), this maybe explained by the lower temperature we used during centrifugal evaporation–drying process.

However, the accuracy of MALDI generated data was lower than ESI–MS/MS data, particularly at lower masses. ESI–MS/MS, which has been successfully applied in proteolytic mapping/sequence analysis of peptides, provides selectivity and structural information (Flamini and De Rosso 2006; Tomás et al. 2008) to validate MALDI spectra. Thus, in the present study, a comprehensive application of MALDI–TOF and ESI–MS/MS helped identify peptide fragments that may arise from hPTH (1–34) inactivation in rat tissue.

As concluded from the analysis of MALDI–TOF and ESI–MS/MS data, a scheme for the hPTH (1–34) degradation mechanism is shown in Fig. 9. The peptide is first cleaved by an endopeptidase, C-terminal to the Leu-residue. The two major degradation products, hPTH (1–15) and hPTH (16–34), are broken down further by exopeptidases. The degradation pattern of hPTH (1–34) in the three rat tissue homogenates was similar, with pronounced cleavage at positions (15–16), (3–4) and (33–34). Some minor differences in the secondary cleavage pattern were also detected. Putative primary degradants and secondary degradants were further metabolized over time. The number of cleavage sites identified was greatest in kidney, with a similar number of sites identified in the liver and lung. This may, in part, result from the differences in protease distribution among the tissues tested. It remains to be determined whether hPTH (1–15), hPTH (16–34), hPTH (1–33) and hPTH (4–34) fragments, which are common to all tissue tested, can be identified in vivo.

It is considered that hydrophilic drugs are rather degraded by soluble enzymes occurring in the blood and membrane bound enzymes than by enzymes that occur mainly or exclusively in the cytoplasma. It also has to be considered that some proteolytic enzymes occur exclusively in liver, kidney or other tissues. To identify the influence of these organs on enzymatic degradation, homogenates of liver or kidney can be used for enzymatic stability studies (Powell et al. 1992; Boulanger et al. 1992). We would like to acknowledge the limitation of our study. Therapeutic peptides and proteins are commonly hydrophilic molecules which will be digested to a much higher extent by such homogenates (containing large amounts of cytosolic enzymes) than can be expected under in vivo conditions. Then, further study in vivo is needed to confirm these results.

In summary, we combined MALDI–TOF MS and LC–ESI–MS/MS technologies to characterize the degradation of hPTH (1–34) in rat kidney, liver and lung homogenates in vitro. We found that the hPTH (1–34) degradation patterns are largely overlapping in the three biological matrices, and the major degradation product results from cleavage of the Leu15–Asn16 peptide bond. These results indicate that amino acid specific proteolytic processing of hPTH (1–34) occurs in all three tissue homogenates. In addition, the sensitivity of degradation to specific inhibitors of serine and metalloproteases suggests that hPTH (1–34) processing occurs by similar proteases in all three tissue homogenates tested here.

**Acknowledgments** This work was supported by grants from The National Key Technologies R&D Program for New Drugs of China (No. 2009ZX09301-002, 2009ZX09503-015 and 2009ZX09304-004).

## References

Boulanger L, Roughly P, Gaudreau P (1992) Catabolism of rat growth hormone-releasing factor (1–29) amide in rat serum and liver. Peptides 13:681–689

Chu NN, Li XN, Chen WL, Xu HR (2007) Pharmacokinetics and safety of recombinant human parathyroid hormone (1–34) (teriparatide) after single ascending doses in Chinese healthy volunteers. Pharmazie 62:869–871

Daugaard H, Egfjord M, Lewin E, Olgaard K (1994a) Metabolism of N-terminal and C-terminal parathyroid hormone fragments by isolated perfused rat kidney and liver. Endocrinology 134:1373–1381

Daugaard H, Egfjord M, Lewin E, Olgaard K (1994b) Metabolism of intact PTH by isolated perfused kidney and liver from uremic rats. Exp Nephrol 2:240–248

Ekins S, Ring BJ, Grace J, McRobie-Belle DJ, Wrighton SA (2000) Present and future in vitro approaches for drug metabolism. Pharmacol Toxicol Methods 44:313–324

Flamini R, De Rosso M (2006) Mass spectrometry in the analysis of grape and wine proteins. Expert Rev Proteom 3:321–331

Föger F, Kopf A, Loretz B, Albrecht K, Bernkop-Schnürch A (2008) Correlation of in vitro and in vivo models for the oral absorption of peptide drugs. Amino Acids 35:233–241

Fraenkel L, Gulanski B, Wittink D (2007) Patient willingness to take teriparatide. Patient Educ Couns 65:237–244

Galluppi GR, Rogge MC, Roskos LK, Lesko LJ, MD Green, Feigal DW Jr (2001) Integration of pharmacokinetic and pharmacodynamic studies in the discovery, development, and review of protein therapeutic agents: a conference report. Clin Pharmacol Ther 69:387–399

Hamdy R (2002) Osteoporosis, the deafening silent epidemic. South Med J 95:567–568

Hu Z, Niu H, Yang X, Li H, Sang G, Li B (2006) Recombinant human parathyroid hormone 1–34: pharmacokinetics, tissue distribution and excretion in rats. Int J Pharm 317:144–154

John H, Walden M, Schäfer S, Genz S, Forssmann WG (2004) Analytical procedures for quantification of peptides in pharmaceutical research by liquid chromatography–mass spectrometry. Anal Bioanal Chem 378:883–897

Jones KO, Owusu-Ababio G, Vick AM, Khan MA (2006) Pharmacokinetics and hepatic extraction of recombinant human parathyroid hormone, hPTH (1–34), in rat, dog, and monkey. J Pharm Sci 95:2499–2506

Liao S, Zhang ZQ, Ruan JX, Qi JK, Liu KL (2008) Degradation of salmon calcitonin in rat kidney and liver homogenates. Pharmazie 63:743–747

Neuman WF, Neuman MW, Sammon PJ, Simon W, Lane K (1975) The metabolism of labeled parathyroid hormone. III. Studies in rats. Calcif Tissue Res 18:251–261

Pezeshki A, Vergote V, Van Dorpe S, Baert B, Burvenich C, Popkov A, De Spiegeleer B (2009) Adsorption of peptides at the sample drying step: influence of solvent evaporation technique, vial material and solution additive. J Pharm Biomed Anal 49:607–612

Potetinova Z, Barbier JR, Suen T, Dean T, Gardella TJ, Willick GE (2006) C-terminal analogues of parathyroid hormone: effect of C-terminus function on helical structure, stability, and bioactivity. Biochemistry 45:11113–11121

Powell MF, Grey H, Gaeta F, Sette A, Colon S (1992) Peptide stability in drug development: a comparison of peptide reactivity in different biological media. J Pharm Sci 81:731–735

Quattrocchi E, Kourlas H (2006) Teriparatide: a review. Clin Ther 26:841–854

Reeve J (2002) Recombinant human parathyroid hormone. BMJ 324:435–436

Seeman E, Compston J, Adachi J, Brandi ML, Cooper C, Dawson-Hughes B, Jönsson B, Pols H, Cramer JA (2007) Noncompliance: the Achilles' heel of anti-fracture therapy. Osteoporos Int 18:711–719

Tomás R, Klepárník K, Foret F (2008) Multidimensional liquid phase separations for mass spectrometry. J Sep Sci 31:1964–1979

Van den Broek I, Sparidans RW, Schellens JH, Beijnen JH (2008) Quantitative bioanalysis of peptides by liquid chromatography coupled to (tandem) mass spectrometry. J Chromatogr B 872:1–22

Vergote V, Van Dorpe S, Peremans K, Burvenich C, De Spiegeleer B (2008) In vitro metabolic stability of obestatin: kinetics and identification of cleavage products. Peptides 29:1740–1748

Werle M, Bernkop-Schnurch A (2006) Strategies to improve plasma half life time of peptide and protein drugs. Amino Acids 30:351–367